A Random Access Control Scheme for a NOMA-Enabled LoRa Network

Wei Wu[1,2], Wennai Wang[1,2(✉)], Jihai Yang[1], and Bin Wang[1,2]

[1] Nanjing University of Posts and Telecommunications, Nanjing, China
wangwn@njupt.edu.com

[2] Key Laboratory of Broadband Wireless Communication and Sensor Network Technology, Ministry of Education, Nanjing, China

Abstract. LoRa is one of the most prominent Low-Power Wide-Area Network (LPWAN) technologies, to accommodate pervasive Internet-of-Things (IoT) connectivities. However, its service capacity and scalability are limited due to the scarce channel resources and the Aloha-like random access mechanism specified by LoRaWAN. We propose a NOMA-enabled LoRa gateway, which permits multiple end-devices to transmit their data at the same time over a shared channel. The whole random access process are provided in detail, including collision resolution and transmission scheduling based on a Distributed Queuing (DQ) method. In addition to that, Spreading Factor (SF) allocation in the transmission scheduling phase is also considered and an optimal problem is formulated to achieve maximum data transmission rate. In order to solve the problem efficiently, an SF allocation algorithm is developed based on the matching theory. Numerical results show that our proposed scheme significantly enhances the sum achievable user rate when the number of users increases.

Keywords: LoRa · Distributed queueing · Non-orthogonal multiple access · Spreading factor allocation · Optimal solution

1 Introduction

Internet of Things (IoT) is a world wide network with pervasive interconnected smart devices [1,2]. It requires advanced technologies, like low-power wide-area Networks (LPWANs), to enable energy-efficient long-range communications. Among LPWAN technologies, LoRa is widely adopted [3].

LoRa is based on chirp spread spectrum (CSS) modulation and spreading factor (SF) is one of the most important transmission parameters. Six SFs (7–12) are available, among which smaller SFs provide higher data rates but reduced ranges, and vise versa. On top of LoRa Physical (PHY) layer, LoRaWAN defines the system architecture and upper layers [5]. The architecture is a star-of-stars topology where gateways (GWs) transparently relay the messages from end-devices (EDs) to network server (NS). The medium access control (MAC) layer protocol is based on Aloha.

H. Gao et al. (Eds.): ChinaCom 2020, LNICST 352, pp. 403–420, 2021.
https://doi.org/10.1007/978-3-030-67720-6_28

The service capacity and scalability of LoRa networks depend on available channel resources and random access mechanism. On one hand, the SF-domain provides another channel resource domain for LoRa, apart from the time- and frequency-domain, since the orthogonality of SFs were demonstrated theoretically [4]. Multiple users can access to the shared time-frequency channel simultaneously using different SFs. However, the number of usable SFs is limited and in practice their complete orthogonality can not be ensured [6]. On the other hand, the throughput performance of Aloha-like MAC protocol is notorious under high traffic load [3], which is directly responsible for LoRa's scalability issue.

With short supply of channel resources, non-orthogonal multiple access (NOMA) has potential to enhance spectral efficiency and support massive connectivity by multiplexing users in power- or code-domain [1]. For the power-domain NOMA, superposition coding (SC) and successive interference cancellation (SIC) are employed to code and decode multiple users' signals. We focus on the power-domain NOMA, which is simply called NOMA later in this paper. In the view of the random access mechanisms, distributed queuing (DQ) is an alternative to Aloha due to its stable and scalable performance in densely loaded networks [9,10].

With that in mind, we propose to leverage the advantages of NOMA and DQ technologies in LoRa networks, in order to address the scalability issue and improve the service capacity. In our NOMA-enabled LoRa network, the gateway coordinates users' contention resolution and data transmission based on a DQ method, and it is NOMA-enabled to permits multiple users to overlap their signals on a shared channel. We firstly provide the whole random access process in detail, including the collision resolution and transmission scheduling. Then, we consider the SF assignment problem for the transmission scheduling phase and formulate it as a maximization problem of achievable rate, under the constraints of inter-SF and successive interferences. For the mathematical intractability of the optimization problem, we propose an SF allocation algorithm based on matching theory.

The remainder of this paper is organized as follows. Section 2 reviews the related works. Section 3 describes the DQ-based access process in details. The SF allocation problem and allocation algorithm are given out in Sect. 4. Numerical results are shown in Sect. 5. Finally, conclusions are made in Sect. 6.

2 Related Works

NOMA has been applied to LPWANs for improving system performance [1,2,7,8]. Authors in [1] model the uplink NOMA in LPWAN and demonstrate that by employing their proposed resource allocation algorithm NOMA can significantly enhance LPWAN. Authors in [2,7,8] leverage NOMA in the context of NB-IoT. [2] proposed a user clustering scheme for a power-domain NOMA aided NB-IoT system, while [7] focuses on the subcarrier and power allocation to maximize the connection density of NB-IoT systems with NOMA. [8] developed an access algorithm that features cluster-based reusable preamble allocation, to enhance the access efficiency for NB-IoT networks.

DQ protocol is first introduced by Xu and Campbell for cable TV distribution [9]. This basic protocol mechanism has been extended to LPWANs with large number of devices [11–13]. [11] proposed a highly-efficient low-power MAC protocol (LPDQ) for wireless data collection scenarios, while [12] and [13] designed DQ-based protocols for crowdsourcing LPWAN and LoRa, respectively. All these works show high throughput regardless of the number of connected devices, due to DQ's stable and scalable performance for densely loaded networks.

Besides, various SF allocation algorithms have been proposed for different objectives, namely, avoiding near-far problems [15], improving network performance [16], enhancing energy efficiency [17], and throughput fairness [18,19]. Among them, the schemes in [17–19] are based on matching theory.

3 Random Access Scheme

3.1 DQ Basics

DQ protocol is based on tree-split algorithm, in which contention resolution and data transmission are separated into two phases: At first, active devices (i.e., the devices who have data to transmit) contend the shared channel by sending short access request (AR). Then, successful devices are allowed to transmit their data in order, whereas collided devices wait for subsequent contention resolution. To inform the devices about the state of each contention, a central coordinator is usually required to broadcast feedback information. Therefore, the frame structure is divided into three parts: (i) m minislots for collision resolution, (ii) one data slot (DS) for uplink collision-free data transmission, and (iii) one feedback slot for downlink feedback information.

Besides, there are two logical queues to manage the collided and successful devices, collision resolution queue (CRQ) and data transmission queue (DTQ). The rules are as follows. The devices that collide in the same CS are organized into one group (called collided group hereafter). All the collided devices are split into different groups and queued into CRQ. Whereas, each successful device enters into one position of the DTQ, waiting for collision-free data transmission. More details about DQ can be found in [9].

3.2 Random Access Process

We consider a NOMA-enabled LoRaWAN system with one GW and N EDs, as depicted in Fig. 1. The GW is located at the center of the cell whose radius is R km, and the EDs randomly distributed in it. One SF can be reused by two or more EDs multiplexed in the power-domain. The sets of EDs and available SFs are denoted by $\mathcal{N} = \{1, 2, ..., N\}$ and $\mathcal{S} = \{7, 8, ..., 12\}$, respectively.

The MAC layer access scheme in our NOMA-enabled LoRa network is developed based on DQ mechanism. Note that the rules of DTQ in this paper is a bit different from the native DQ, since multiple users' data streams can be transmitted in the same DS by combining the power- and SF-domain resources.

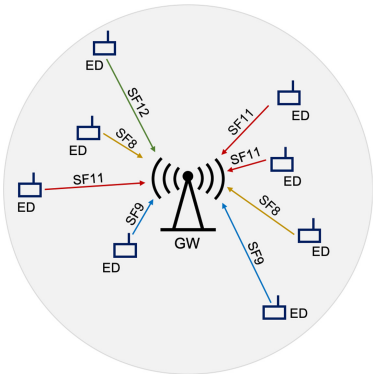

Fig. 1. A NOMA-enabled LoRa network, where multiple EDs use the same SF channel in power-domain and multiple SFs are used simultaneously.

The modified rules are as follows. Among the successful devices in one minislot, some of them are allowed to transmit in the same DS and they are organized into one group (called successful group later). Each successful group enters into one position of DTQ. For that, the feedback information should also indicate, apart from the state of each CS, the allocated SF for each successful ED and whether it is permitted to transmit in the next frame.

Figure 2 shows an example to illustrate the whole random access process. In this example, there are ten EDs and one GW, and three available SFs (SF7–9). Besides, we make two assumptions: (i) Six contention slots (CSs) are set in each contention window (CW). Since the speed of collision resolution is faster than data transmission in native DQ when three or more CSs are used [10], it is reasonable to set more CSs when multiple users' data can be transmitted in one DS. (ii) Each SF can be assigned to at most two EDs. More number of users' signals superimposed will increase the complexity of receiver.

- **Synchronization:** a beacon period starts after the GW broadcasts a beacon (BCN) signal. Ten active devices (ED1–10) are synchronized and switch to Class B mode.
- **Superframe 1:** all the devices contend in the CW by sending ARs. ED3, 5, 6, and 9 succeed in the second, forth, fifth and sixth CS respectively, while others collide. After that, the GW broadcasts feedback (FB) in the FS. Note that there is no data transmission in this frame because DTQ is empty at that time. All the devices receive the FB.
  Two collided groups ($\{1, 4, 7, 8\}$ and $\{2, 10\}$) enter into the first two positions of CRQ, while two successful groups ($\{3, 5, 6\}$ and $\{9\}$) enter into the first two positions of DTQ. Note that although ED9 succeeds in this CW, it queues in the second position since it is not allowed to transmit in the next frame.
- **Superframe 2:** the first group in the CRQ (ED1, 4, 7 and 8) contend in the CW and they both succeed. The first group in the DTQ (ED3, 5 and 6) transmit their data using assigned SFs in the DS. GW broadcasts FB in the FS.

ED1, 4, 7 and 8 are allowed to transmit in the next superframe and enter into the first position of DTQ.

- **Superframe 3:** ED2 and 10 contend in the CW. Subsequently, ED1, 4, 7, 8 and 9 transmit data using different SFs. GW still broadcasts FB in the FS. ED2 and 10 enter into the first position of DTQ.
- **Superframe 4:** the CW is empty since the CRQ is empty at that time. Then, ED2 and 10 transmit data in the DS, and the GW broadcasts FB in the FS.

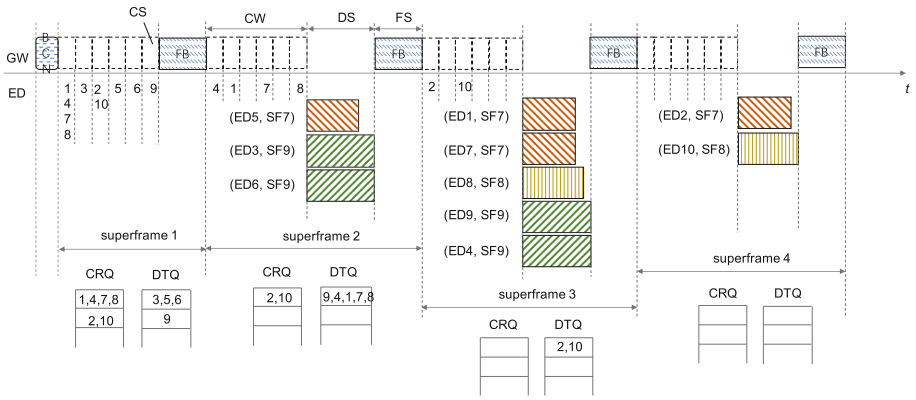

Fig. 2. An example to illustrate the random access process in the NOMA-enabled LoRa network.

4 Spreading Factor Allocation

4.1 Problem Formulation

For each ED n assigned to SF s, it would be impaired by (one of) two kinds of interferences: (a) inter-SF interference, caused by the EDs using SF j ($j \neq s$); (b) co-SF interference, resulting from the EDs using SF s. Note that when the NOMA-enabled GW performs SIC, the strongest signal is decoded at first from the composite received signal and then it will be reconstructed and subtracted from the received signal, after that, the next strongest and so on. Therefore, among the co-SF interferences, only the EDs with lower received power than ED n will affect ED n's reception, which is called successive interference. So that we consider inter-SF (θ_s) and successive interferences in this paper, and the inter-SF and SIC (μ) capture thresholds are listed in Table 1 [19,22].

The channel gain between ED n ($n \in \mathcal{N}$) and the GW, considering both path-loss and small-scale fading, can be expressed as,

$$h_n = \frac{|g_n|^2 \, \mathrm{A}(f_c)}{d_n^{\alpha}}, \tag{1}$$

Table 1. Inter-SF and SIC capture thresholds

SF	7	8	9	10	11	12
Inter-SF threshold θ_s (dB)	-7.5	-9	-13.5	-15	-18	-22.5
SIC threshold μ (dB)	6					

where g_n, f_c, d_n, and α are the small-scale channel fading gain, carrier frequency, distance between ED n and the GW, and path-loss exponent, respectively. $\mathrm{A}(f_c) = (f_c^2 \times 10^{-2.8})^{-1}$, is the deterministic path-loss term [19].

Then, the signal-to-interference-plus-noise-ratio (SINR) can be expressed as,

$$\mathrm{SINR}_{ns} = \frac{p_n \gamma_n}{I_{\mathrm{iSF}} + I_{\mathrm{SI}} + 1}, \tag{2}$$

where p_n is the transmit power of ED n and $\gamma_n = h_n/\sigma_c^2$, where σ_c^2 is the power of additive white gaussian noise. I_{iSF} and I_{SI} are the power of inter-SF and successive interferences, which can be expressed as

$$I_{\mathrm{iSF}} = \sum_{j \in \mathcal{S} \setminus \{s\}} \sum_{i \in \mathcal{N} \setminus \{n\}} x_{ij} p_i \gamma_i, \tag{3}$$

$$I_{\mathrm{SI}} = \sum_{i=n+1}^{|\mathcal{U}_s|} x_{is} p_i \gamma_i, \tag{4}$$

where x_{ij} is an indicator variable for SF assignment, 1 when ED i assigned to SF j and 0 otherwise. $\mathcal{U}_s$ is the set of EDs assigned to SF s, and they are sorted according to the descending order of received power. Considering Rayleigh fading channels, γ_n can be modeled as an exponential random variable with mean $\bar{\gamma}_n = \mathrm{A}(f_c)/(d_n^{\alpha}\sigma_c^2)$ [19].

It is worth to mention that Eq. (2) is a general SINR expression. In some cases, the I_{iSF} or I_{SI} term not exists. For the detailed expression, there are three cases when $N > 1$ (let $|\mathcal{S}_A| > 1$ denotes the set of used SFs):

- **Case 1:** $|\mathcal{S}_A| > 1$ and $|\mathcal{U}_s| = 1$. ED n is only impaired by inter-SF interference, i.e., $\mathrm{SINR}_{ns}^{(\mathrm{case1})} = p_n\gamma_n/(I_{\mathrm{iSF}} + 1)$. Therefore, its transmission can be successfully decoded if it satisfies the inter-SF capture condition and signal reception condition.
- **Case 2:** $|\mathcal{S}_A| = 1$ and $|\mathcal{U}_s| > 1$. ED n is only impaired by successive interference, i.e., $\mathrm{SINR}_{ns}^{(\mathrm{case2})} = p_n\gamma_n/(I_{\mathrm{SI}} + 1)$. The transmission can be successfully decoded if ED n satisfies the SIC and signal reception conditions.
- **Case 3:** $|\mathcal{S}_A| > 1$ and $|\mathcal{U}_s| > 1$. ED n is subject to both inter-SF and successive interferences, i.e., $\mathrm{SINR}_{ns}^{(\mathrm{case3})} = p_n\gamma_n/(I_{\mathrm{iSF}} + I_{\mathrm{SI}} + 1)$. The transmission can be successfully decoded when the inter-SF, SIC, and signal reception conditions are all satisfied.

According to [20], the relationship of these three conditions is "SIC capture threshold> SIC threshold> reception condition".

As the access process shown in Fig. 2, SF allocation should be performed every superframe, during which the path-loss term can be assumed to be fixed. Therefore, we consider achievable short-term average rate when formulate the SF allocation problem. The achievable short-term average rate (simply achievable rate hereafter) is defined as the multiplication of successful probability and data bitrate [20], i.e.,

$$\mathrm{AR}_{ns} = R_s \times P_{ns}, \tag{5}$$

where P_{ns} is the probability of successful reception and $R_s = (s \cdot \mathrm{CR} \cdot \mathrm{BW})/2^s$ is the data bitrate, where BW is the bandwidth and CR is the coding rate. In LoRa, there are three typical bandwidths (125, 250, and 500 kHz) and four coding rates (4/5, 4/6, 4/7, and 4/8) [14].

In the first case, the successful probability is,

$$P_{ns}^{(\mathrm{case1})} = P\left(\mathrm{SINR}_{ns}^{(\mathrm{case1})} \geq \theta_s\right), \tag{6}$$

According to [19], Eq. (6) can be written as,

$$P_{ns}^{(\mathrm{case1})} = e^{-\frac{\theta_s \sigma_c^2 d_n^2}{\mathrm{A}(f_c) p_n}} \prod_{j \in \mathcal{S}\setminus\{s\}} \prod_{i \in \mathcal{N}\setminus\{n\}} \frac{1}{\theta_s x_{ij} \frac{p_i}{p_n} \left(\frac{d_n}{d_i}\right)^{\alpha} + 1}. \tag{7}$$

In the second case, the successful probability is changed to,

$$P_{ns}^{(\mathrm{case2})} = P\left(\mathrm{SINR}_{ns}^{(\mathrm{case2})} \geq \mu\right), \tag{8}$$

We derive $P_{ns}^{(\mathrm{case2})}$ with similar calculations as in [19] (see Appendix 1),

$$P_{ns}^{(\mathrm{case2})} = e^{-\frac{\mu \sigma_c^2 d_n^2}{\mathrm{A}(f_c) p_n}} \prod_{i=n+1}^{|\mathcal{U}_s|} \frac{1}{\mu x_{is} \frac{p_i}{p_n} \left(\frac{d_n}{d_i}\right)^{\alpha} + 1}. \tag{9}$$

In the last case, the successful probability is,

$$P_{ns}^{(\mathrm{case3})} = P\left(\mathrm{SINR}_{ns}^{(\mathrm{case3})} \geq \mu\right), \tag{10}$$

which can be written as (see Appendix 2),

$$\begin{aligned} P_{ns}^{(\mathrm{case3})} = & e^{-\frac{\mu \sigma_c^2 d_n^2}{\mathrm{A}(f_c) p_n}} \prod_{j \in \mathcal{S}\setminus\{s\}} \prod_{i \in \mathcal{N}\setminus\{n\}} \frac{1}{\mu x_{ij} \frac{p_i}{p_n} \left(\frac{d_n}{d_i}\right)^{\alpha} + 1} \\ & \times \prod_{i=n+1}^{|\mathcal{U}_s|} \frac{1}{\mu x_{is} \frac{p_i}{p_n} \left(\frac{d_n}{d_i}\right)^{\alpha} + 1}. \end{aligned} \tag{11}$$

Given the above analysis, the general expression of successful probability can be written as,

$$\begin{aligned} P_{ns} =& \mathrm{I}\left(|\mathcal{S}_A| > 1, |\mathcal{U}_s| = 1\right) \times P_{ns}^{(\text{case1})} \\ &+ \mathrm{I}\left(|\mathcal{S}_A| = 1, |\mathcal{U}_s| > 1\right) \times P_{ns}^{(\text{case2})} \\ &+ \mathrm{I}\left(|\mathcal{S}_A| > 1, |\mathcal{U}_s| > 1\right) \times P_{ns}^{(\text{case3})} \end{aligned} \tag{12}$$

where $\mathrm{I}(*)$ is an indicator function, 1 when the condition $(*)$ is verified and 0 otherwise.

Finally, the SF allocation optimization problem is formulated as follows,

$$(\mathrm{P}) \max \sum_{s\in\mathcal{S}} \sum_{n\in\mathcal{N}} x_{ns} \mathrm{AR}_{ns} \tag{13a}$$

$$\text{s.t.} \quad \mathrm{C1}: \sum_{s\in\mathcal{S}} x_{ns} \leq 1, \quad \forall n \in \mathcal{N} \tag{13b}$$

$$\mathrm{C2}: \sum_{n\in\mathcal{N}} x_{ns} \leq \lambda_s, \quad \forall s \in \mathcal{S} \tag{13c}$$

$$\mathrm{C3}: x_{ns} = \{0, 1\}, \quad \forall n \in \mathcal{N}, \forall s \in \mathcal{S} \tag{13d}$$

where λ_s is the maximal number of EDs that can be allocated to SF s. Our objective function is the maximization of sum achievable rate of all served EDs (i.e., $\sum_{s\in\mathcal{S}} x_{ns} \neq 0, \forall n \in \mathcal{N}$). Constraints C1 ensures that an ED n is assigned to at most one SF, while C2 makes that the maximal number of EDs sharing SF s is λ_s. Constraint C3 defines the binary SF allocation variable x_{ns}.

4.2 Proposed SF Allocation Algorithm

For simplicity, we assume that $p_n = p_0$ $(\forall n \in \mathcal{N})$, then the optimization problem (P) is an integer programming problem with a non-linear objective function, which is difficult to obtain its optimal solution. Therefore, we propose an SF allocation algorithm based on matching theory [21], which is a promising tool for resource allocation in wireless networks. According to the matching theory, our allocation problem (P) is classified as a many-to-one matching problem with conventional externalities and peer effects. The basic concepts of the matching theory that have been used in our algorithm are listed in Table 2.

The steps of our proposed SF allocation algorithm are as follows.

Initialization: the preference lists of EDs and SFs are initialized at first. The preference list of ED n is,

$$\mathcal{PL}_n = \{s \in \mathcal{S}, \text{s.t. } d_n \leq l_s\}, \tag{14}$$

where l_s is the distance threshold of SF s, and $\mathcal{PL}_n$ is arranged according to the ascending order of l_s. We assume that all EDs are in the coverage area of the largest SF, hence $\mathcal{PL}_n \neq \emptyset$ $(\forall n \in \mathcal{N})$.
The preference list of SF s is,

$$\mathcal{PL}_s = \{n \in \mathcal{N}, \text{s.t. } d_n \leq l_s\}. \tag{15}$$

Table 2. Basic concepts used in our algorithm

Concept name	Definition
Matching pair	A couple (n, s) assigned to each other
Quota of a player	The maximum number of players with which it can be matched. Each ED has a quota of 1 and each SF s has a quota of λ_s
Utility of an ED n	The achievable rate of ED n, i.e., $f_n = R_s \times P_{ns}$
Utility of an SF s	The sum achievable rate of the EDs assigned to SF s, i.e., $f_s = \sum_{n \in \mathcal{U}_s} R_s \times P_{ns}$
Preference relation	For ED n, it prefers SF s_1 over SF s_2, if the utility of n is higher when it is matched to s_1 than when it is matched to s_2. For an SF, the criterion is same
Blocking pair	A matching pair (n, s) which makes new utility $\sum_{s \in \mathcal{S}} f'_s$ higher than the current utility $\sum_{s \in \mathcal{S}} f_s$. In this case, n will leave its current match to make pair with s
Two-sided exchange stable matching	A matching solution where there is no blocking pair

$\mathcal{PL}_s$ is arranged in the ascending order of d_n. Unmatched devices are added to $\mathcal{L}_u$.

Initial Matching: for each ED n in the unmatched list $\mathcal{L}_u$, it is removed from $\mathcal{L}_u$ whenever it starts requesting the first SF in $\mathcal{PL}_n$. If the quota of the kth $(1 \leq k \leq |\mathcal{PL}_u|)$ SF allows it to accept the request, ED n is matched to this SF and stops requesting, otherwise it moves to request the $(k+1)$th SF. If ED n is not accepted by any SF in $\mathcal{PL}_n$, it is added into the set $\mathcal{L}_{ru}$. The process is repeated until $\mathcal{L}_u$ becomes empty.

SF Matching Refinement: for each matching pair (n, s), the algorithm calculates $\sum_{s \in \mathcal{S}} fs$. Firstly, if there exists an SF k whose quota allows it to accept n, the algorithm makes new pair (n, k) and calculates the new utility $\sum_{s \in \mathcal{S}} fs'$. If $\sum_{s \in \mathcal{S}} fs' > \sum_{s \in \mathcal{S}} fs$, ED n leaves SF s to be matched with SF k. Then, the algorithm makes a swap between every matched pair (m, k) and (n, s). If (n, k) or (m, s) is a blocking pair, the swap is validated. This swapping step is repeated until reaching a two-sided stable matching.

Algorithm 1. Initial Matching

Initialization: $\mathcal{L}_u \leftarrow \mathcal{N}, \mathcal{L}_{ru} \leftarrow \emptyset$.

while $\mathcal{L}_u \neq \emptyset$ **do**
  for $i \in \mathcal{L}_u$ **do**
    $\mathcal{L}_u \leftarrow \mathcal{L}_u \backslash \{i\}$;
    $c = 1$;
    while $\sum_{j \in \mathcal{S}} x_{ij} < 1$ and $c \leq |\mathcal{PL}_i|$ **do**
      $j \leftarrow$ the cth SF in $\mathcal{PL}_i$;
      if $|\mathcal{U}_j| < \lambda_j$ **then**
        $x_{ij} = 1$;
        $\mathcal{U}_j \leftarrow \mathcal{U}_j \cup \{i\}$;
      else
        $c = c + 1$;
    if $\sum_{j \in \mathcal{S}} x_{ij} = 0$ **then**
      $\mathcal{L}_{ru} \leftarrow \mathcal{L}_{ru} \cup \{i\}$;

User Matching Refinement (when $\mathcal{L}_{ru} \neq \emptyset$): Firstly, for each ED i in $\mathcal{L}_{ru}$ and an SF j ($j \in \mathcal{PL}_i$) whose quota allows it to accept ED i, the algorithm makes a new pair (i, j). If (i, j) makes the new utility $\sum_{s \in \mathcal{S}} fs'$ higher, the new pair is validated. Then, for each SF l ($l \in \mathcal{PL}_i$) whose quota not allows it to accept ED i, the algorithm makes a swap between every (k, l) ($k \in \mathcal{U}_l$) and $(i, \emptyset)$. If (i, l) is a blocking pair, the swap is validated. This swapping step is repeated until reaching a two-sided stable matching.

Complexity: The running time of our proposed SF allocation algorithm is upper bounded by $\mathcal{O}\left(\lambda_{\max}^2 S^2 + (1 + \lambda_{\max})NS\right)$, where $\lambda_{\max} = \max_{s \in \mathcal{S}} \lambda_s$.

Proof. (i) Initial matching complexity: in the worst case, every ED has the same preference list including all the SFs and it has to search until the last one in its preference list. Therefore, the complexity of the initial matching is upper bounded by $\mathcal{O}(NS)$.
(ii) SF matching refinement complexity: for each SF s, the algorithm considers at most λ_s assigned EDs and examines $\sum_{j \in \mathcal{S} \backslash \{s\}} \lambda_j$ swap operations for each ED. Then the number of swap operations that are examined in one iteration is upper bounded by $\mathcal{O}\left(\lambda_s \sum_{j \in \mathcal{S} \backslash \{s\}} \lambda_j\right)$. The complexity of the SF matching refinement is upper bounded by $\mathcal{O}\left(\sum_{s \in \mathcal{S}} \left(\lambda_s \sum_{j \in \mathcal{S} \backslash \{s\}} \lambda_j\right)\right)$. Let $\lambda_{\max} = \max_{s \in \mathcal{S}} \lambda_s$, it can be represented as $\mathcal{O}\left(\lambda_{\max}^2 S(S-1)\right)$.
(iii) User matching refinement complexity: in the worst case, each ED n in the set $\mathcal{L}_{ru}$ has the same preference list containing all the SFs, and at most λ_s swap operations are examined for each SF s in ED n's preference list. Hence, in each

Algorithm 2. SF Matching Refinement

change←ture;
while change==ture **do**
  change←false;
  for $j \in \mathcal{S}$ **do**
    for $i \in \mathcal{U}_j$ **do**
      for $l \in \mathcal{S} \backslash \{j\}$ **do**
        if $\mathcal{U}_l == \emptyset$ **then**
          Swap (i, j) and $(\emptyset, l)$;
          if (i, l) is blocking pair **then**
            Validate the swap;
            change←true;
        else
          for $k \in \mathcal{U}_l$ **do**
            Swap (i, j) and (k, l);
            if (i, j) or (k, l) is blocking pair **then**
              Validate the swap;
              change←true;

interation the number of swap operations is upper bounded by $\mathcal{O}(\lambda_{\max} S)$. Considering at most N EDs in $\mathcal{L}_{ru}$, the complexity of the user matching refinement is upper bounded by $\mathcal{O}(\lambda_{\max} NS)$.

Therefore, the computational complexity of the SF allocation algorithm is upper bounded by $\mathcal{O}\left(\lambda_{\max}^2 S^2 + (1 + \lambda_{\max}) NS\right)$.

Table 3. Simulation parameters

Carrier frequency (f_c)	868 MHz
Bandwidth (BW)	125 kHz
ED transmit power (p_0)	14 dBm
Cell radius (R)	1 km
Path loss exponent (α)	4
Available SFs	7–12
Quota of each SF s (λ_s)	2

5 Numerical Results

We consider two baseline schemes for performance comparison with our proposed SF allocation scheme.

- **Random SF allocation:** for each ED n, it randomly requests a usable SF (i.e., the SFs in its preference list), and the SF accepts the request if its quota allows. The process stops untill ED n has been matched with an SF, or all the usable SFs has been requested.

Algorithm 3. User Matching Refinement

change←ture;
while change==ture **do**
  change←false;
  for $i \in \mathcal{L}_{ru}$ **do**
    for $j \in \mathcal{PL}_i$ **do**
      Calculate $\sum_{s \in \mathcal{S}} f_s$;
      if $|\mathcal{U}_j| < \lambda_j$ **then**
        Make the new pair (i, j);
        Calculate the new utility $\sum_{s \in \mathcal{S}} f'_s$;
        if $\sum_{s \in \mathcal{S}} f'_s \geq \sum_{s \in \mathcal{S}} f_s$ **then**
          Validate the new pair;
          change←true;
      else
        for $k \in \mathcal{U}_j$ **do**
          Swap $(i, \emptyset)$ and (k, j);
          if (i, j) is blocking pair **then**
            Validate the new pair;
            change←true;

– **Distance SF allocation:** for each ED n, it requests the usable SFs in order, from the smallest to the largest SF. The process stops untill ED n has been matched with an SF, or all the usable SFs has been requested.

Simulation parameters are set under European regulations, shown in Table 3. Note that we consider a lossy urban environment with path loss exponent 4.

The performance comparison of our proposed scheme and the baseline schemes are shown in Fig. 3, where the sum achievable rate and the number of served EDs are plotted, against the number of EDs. We can observe from Fig. 3(a) that our proposed algorithm outperforms the baseline algorithms regardless of the number of devices. The reason is that our algorithm considers the effects of interferences (both inter-SF and successive interferences) and tries to suppress them by careful SF assignment. Note that all the curves become flat when $N \geq 16$, which can be explained by Fig. 3(b). The number of served devices under the random and distance algorithms reach the maximum served devices (12) when $N \geq 16$, whereas that under the proposed algorithm keeps around 8. The results are rational since the proposed scheme exhausts itself suppressing the interferences rather than serving users. The relationship between the number of EDs and the served EDs would give instructions to the optimal number of CSs setting in each CW.

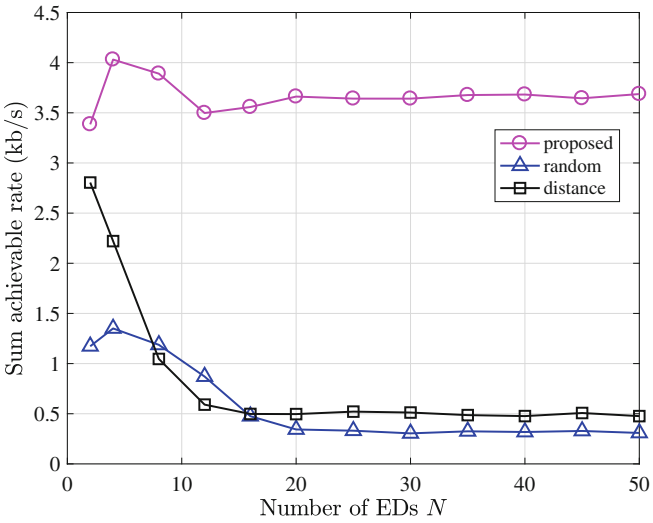

(a)

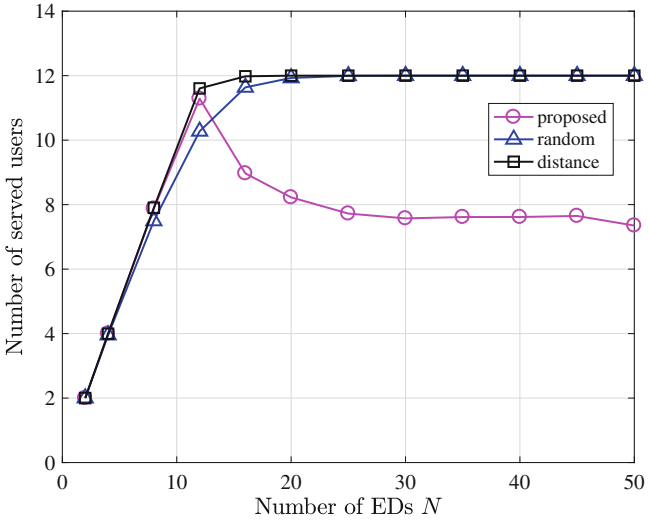

(b)

Fig. 3. Performance comparison between the proposed SF allocation scheme and baseline schemes. (a) Sum achievable rate. (b) Number of served users.

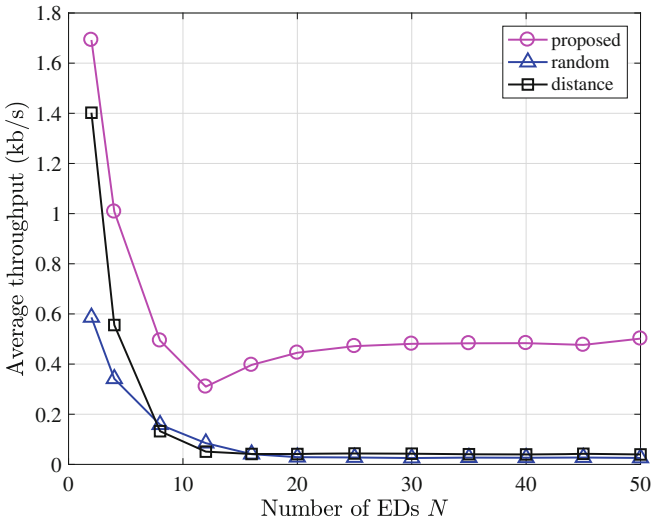

Fig. 4. Average throughput.

When $4 < N < 16$, the sum achievable rate under the distance algorithm is slightly higher than the random one. The reason is that the distance algorithm tries to allocate the smallest available SF for each ED, which makes (i) smaller gap between the used SFs, and (ii) a higher probability that one SF is assigned to more than one device. Therefore, interference rises in the distance algorithm case. However, the sum achievable rate under the distance algorithm becomes slightly higher than the random one, when the number of served devices increases. The reason is that devices suffer serious interferences in both baseline algorithms when the served devices increases, but distance algorithm allocate the smallest available SF to each device, making the data rate higher.

Figure 4 shows the average throughput. The average throughput of the proposed scheme first descends with the increasing number of EDs when $N \leq 12$, then it rises slightly and goes flat. The average throughput of the baseline schemes drops fast when $N \leq 12$, after that it keeps around 0.05 kb/s. Our proposed algorithm is superior than the baseline ones. In addition, in terms of the throughput, our proposal is also better than that in [18]. As shown in Fig. 3 of [18], the average throughput of their proposal decreases against the number of nodes and is lower than 0.2 kb/s when the number of nodes is greater than 15. Whereas, our proposal makes the average throughput always higher than 0.3 kb/s.

6 Conclusion

To accommodate massive connectivity in IoT applications, we propose a noval LoRa network combined with NOMA and DQ technologies, in which a NOMA-enabled gateway allows multiple devices to transmit data simultaneously over the shared channel. The whole random access process of EDs is divided into collision resolution and transmission scheduling phases, which is coordinated by the GW based on the DQ mechanism. The details of access process are provided. In addition, an SF allocation algorithm for the transmission scheduling phase is proposed. We first formulate an SF allocation problem under the constraints of inter-SF and successive interferences, then develop the allocation algorithm based on the optimization problem and matching theory. Numerical results show that our SF allocation scheme outperforms the random and distance based schemes.

A Appendix 1

We now prove Eq. (9). Under the assumption of Rayleigh fading, γ_n can be modeled as exponential random variable with mean $\bar{\gamma}_n = \mathrm{A}(f_c)/(d_n^{\alpha}\sigma_c^2)$, then Eq. (8) can be developed as

$$\begin{aligned} P_{ns}^{(\text{case2})} =& P\left(\frac{\gamma_n p_n}{\sum_{i=n+1}^{|\mathcal{U}_s|} x_{is}\gamma_i p_i + 1} \geq \mu \middle| \gamma_{n+1}\cdots\gamma_{|\mathcal{U}_s|}\right) \times P\left(\gamma_{n+1}\cdots\gamma_{|\mathcal{U}_s|}\right) \\ =& \int_{\gamma_{n+1}} \cdots \int_{\gamma_{|\mathcal{U}_s|}} P\left(\gamma_n \geq \frac{\mu}{p_n}\left(\sum_{i=n+1}^{|\mathcal{U}_s|} x_{is}\gamma_i + 1\right)\right) \\ & \times P\left(\gamma_{n+1}\cdots\gamma_{|\mathcal{U}_s|}\right)\, d\gamma_{n+1}\cdots d\gamma_{|\mathcal{U}_s|}. \end{aligned} \tag{16}$$

Let $Z = P\left(\gamma_n \geq \frac{\mu}{p_n}\left(\sum_{i=n+1}^{|\mathcal{U}_s|} x_{is}\gamma_i + 1\right)\right)$, then

$$\begin{aligned} Z &= \int_a^{\infty} p(\gamma_n)\, d\gamma_n = \int_a^{\infty} \frac{1}{\bar{\gamma}_n} e^{-\frac{\gamma_n}{\bar{\gamma}_n}}\, d\gamma_n \\ &= e^{-\frac{\mu\left(\sum_{i=n+1}^{|\mathcal{U}_s|} x_{is}\gamma_i p_i + 1\right)}{\bar{\gamma}_n p_n}}, \end{aligned} \tag{17}$$

where $a = \frac{\mu}{p_n}\left(\sum_{i=n+1}^{|\mathcal{U}_s|} x_{is}\gamma_i p_i + 1\right)$. Substituting Z in Eq. (16), we obtain that

$$\begin{aligned}
P_{ns}^{(\text{case2})} &= \int_{\gamma_{n+1}} \cdots \int_{\gamma_{|\mathcal{U}_s|}} e^{-\frac{\mu\left(\sum_{i=n+1}^{|\mathcal{U}_s|} x_{is}\gamma_i p_i + 1\right)}{\bar{\gamma}_n p_n}} P\left(\gamma_{n+1}\cdots\gamma_{|\mathcal{U}_s|}\right) \\
&\quad \times d\gamma_{n+1}\cdots d\gamma_{|\mathcal{U}_s|} \\
&= e^{-\frac{\mu}{\bar{\gamma}_n p_n}} \prod_{i=n+1}^{\mathcal{U}_s} \int_{\gamma_i} e^{-\frac{\mu x_{is}\gamma_i p_i}{\bar{\gamma}_n p_n}} p(\gamma_i)\, d\gamma_i \\
&= e^{-\frac{\mu}{\bar{\gamma}_n p_n}} \prod_{i=n+1}^{\mathcal{U}_s} \frac{1}{\bar{\gamma}_i} \int_{\gamma_i} e^{-\frac{\mu x_{is}\bar{\gamma}_i p_i + \bar{\gamma}_n p_n}{\bar{\gamma}_n \bar{\gamma}_i p_n}} \gamma_i\, d\gamma_i \\
&= e^{-\frac{\mu}{\bar{\gamma}_n p_n}} \prod_{i=n+1}^{\mathcal{U}_s} \frac{1}{\bar{\gamma}_i} \cdot \frac{\bar{\gamma}_n\bar{\gamma}_i p_n}{\mu x_{is}\bar{\gamma}_i p_i + \bar{\gamma}_n p_n} \\
&\quad \times \int_{\gamma_i} \frac{\mu x_{is}\bar{\gamma}_i p_i + \bar{\gamma}_n p_n}{\bar{\gamma}_n\bar{\gamma}_i p_n} e^{-\frac{\mu x_{is}\bar{\gamma}_i p_i + \bar{\gamma}_n p_n}{\bar{\gamma}_n\bar{\gamma}_i p_n}\gamma_i}\, d\gamma_i \\
&= e^{-\frac{\mu}{\bar{\gamma}_n p_n}} \prod_{i=n+1}^{\mathcal{U}_s} \frac{\bar{\gamma}_n p_n}{\mu x_{is}\bar{\gamma}_i p_i + \bar{\gamma}_n p_n} \\
&= e^{-\frac{\mu\sigma_c^2 d_n^2}{\mathrm{A(fc)pn}}} \prod_{i=n+1}^{\mathcal{U}_s} \frac{1}{\mu x_{is}\frac{p_i}{p_n}\left(\frac{d_n}{d_i}\right)^{\alpha} + 1}.
\end{aligned} \tag{18}$$

B Appendix 2

We derivate Eq. (11) with similar calculations in Appendix 1.

$$\begin{aligned}
P_{ns}^{(\text{case3})} &= P\left(\frac{\gamma_n p_n}{\sum_{j\in\mathcal{S}\setminus\{s\}}\sum_{i\in\mathcal{N}\setminus\{n\}} x_{ij}\gamma_i p_i + \sum_{i=n+1}^{|\mathcal{U}_s|} x_{is}\gamma_i p_i + 1} \geq \mu \,\middle|\, \gamma_1\cdots\gamma_{n-1}\gamma_{n+1}\cdots\gamma_N\right) \\
&\quad \times P\left(\gamma_1\cdots\gamma_{n-1}\gamma_{n+1}\cdots\gamma_N\right) \\
&= \int_{\gamma_1}\cdots\int_{\gamma_N} P\left(\gamma_n \geq \frac{\mu}{p_n}\left(\sum_{j\in\mathcal{S}\setminus\{s\}}\sum_{i\in\mathcal{N}\setminus\{n\}} x_{ij}\gamma_i p_i + \sum_{i=n+1}^{|\mathcal{U}_s|} x_{is}\gamma_i p_i + 1\right)\right) \\
&\quad \times P\left(\gamma_1\cdots\gamma_N\right)\, d\gamma_1\cdots d\gamma_N.
\end{aligned} \tag{19}$$

Let $Z' = P\left(\gamma_n \geq \frac{\mu}{p_n}\left(\sum_{j\in\mathcal{S}\setminus\{s\}}\sum_{i\in\mathcal{N}\setminus\{n\}} x_{ij}\gamma_i + \sum_{i=n+1}^{|\mathcal{U}_s|} x_{is}\gamma_i + 1\right)\right)$,

$$\begin{aligned} Z' &= \int_{a'}^{\infty} \frac{1}{\bar{\gamma}_n} e^{-\frac{\gamma_n}{\bar{\gamma}_n}}\, d\gamma_n \\ &= e^{-\frac{\mu\left(\sum_{j\in\mathcal{S}\setminus\{s\}}\sum_{i\in\mathcal{N}\setminus\{n\}} x_{ij}\gamma_i p_i + \sum_{i=n+1}^{|\mathcal{U}_s|} x_{is}\gamma_i p_i + 1\right)}{\bar{\gamma}_n p_n}}, \end{aligned} \tag{20}$$

where $a' = \frac{\mu}{p_n}\left(\sum_{j\in\mathcal{S}\setminus\{s\}}\sum_{i\in\mathcal{N}\setminus\{n\}} x_{ij}\gamma_i p_i + \sum_{i=n+1}^{|\mathcal{U}_s|} x_{is}\gamma_i p_i + 1\right)$. Substituting Z' in Eq. (19), we obtain

$$\begin{aligned} P_{ns}^{(\text{case3})} &= \int_{\gamma_1}\cdots\int_{\gamma_N} e^{-\frac{\mu\left(\sum_{j\in\mathcal{S}\setminus\{s\}}\sum_{i\in\mathcal{N}\setminus\{n\}} x_{ij}\gamma_i p_i + \sum_{i=n+1}^{|\mathcal{U}_s|} x_{is}\gamma_i p_i + 1\right)}{\bar{\gamma}_n p_n}} \\ &\quad \times P\left(\gamma_1\cdots\gamma_N\right)\, d\gamma_1\cdots d\gamma_N \\ &= e^{-\frac{\mu}{\bar{\gamma}_n p_n}} \prod_{j\in\mathcal{S}\setminus\{s\}}\prod_{i\in\mathcal{N}\setminus\{n\}} \int_{\gamma_i} e^{-\frac{\mu x_{ij}\gamma_i p_i}{\bar{\gamma}_n p_n}} p(\gamma_i)\, d\gamma_i \\ &\quad \times \prod_{i=n+1}^{\mathcal{U}_s} \int_{\gamma_i} e^{-\frac{\mu x_{is}\gamma_i p_i}{\bar{\gamma}_n p_n}} p(\gamma_i)\, d\gamma_i \\ &= e^{-\frac{\mu}{\bar{\gamma}_n p_n}} \prod_{j\in\mathcal{S}\setminus\{s\}}\prod_{i\in\mathcal{N}\setminus\{n\}} \frac{\bar{\gamma}_n p_n}{\mu x_{is}\bar{\gamma}_i p_i + \bar{\gamma}_n p_n} \\ &\quad \times \prod_{i=n+1}^{\mathcal{U}_s} \frac{\bar{\gamma}_n p_n}{\mu x_{is}\bar{\gamma}_i p_i + \bar{\gamma}_n p_n} \\ &= e^{-\frac{\mu\sigma_c^2 d_n^2}{A(f_c)p_n}} \prod_{j\in\mathcal{S}\setminus\{s\}}\prod_{i\in\mathcal{N}\setminus\{n\}} \frac{1}{\mu x_{is}\frac{p_i}{p_n}\left(\frac{d_n}{d_i}\right)^{\alpha} + 1} \\ &\quad \times \prod_{i=n+1}^{\mathcal{U}_s} \frac{1}{\mu x_{is}\frac{p_i}{p_n}\left(\frac{d_n}{d_i}\right)^{\alpha} + 1} \end{aligned} \tag{21}$$

References

1. Li, K., Benkhelifa, F., Mccann, J.: Resource allocation for non-orthogonal multiple access (NOMA) enabled LPWA networks. arXiv: 1908.09336 (2019)
2. Shahini, A., Ansari, N.: NOMA aided narrowband IoT for machine type communications with user clustering. IEEE IoT J. **6**(4), 7183–7191 (2019)
3. Adelantado, F., Vilajosana, X., Tuset-Peiró, P., et al.: Understanding the limits of LoRaWAN. IEEE Commun. Mag. **55**(9), 34–40 (2017)
4. Vangelista, L.: Frequency shift chirp modulation: the LoRa modulation. IEEE Signal Process. Lett. **24**(12), 1818–1821 (2017)
5. LoRa Alliance. V1.0.3. LoRaWANTM Specification (2018)
6. Corce, D., Gucciardo, M., Tinnirello, I., et al.: Impact of spreading factor imperfect orthogonality in LoRa communications. In: Piva, A., Tinnirello, I., Morosi, S. (eds.) Digital Communication. Towards a Smart and Secure Future Internet. CCIS, vol. 766, pp. 165–179. Springer, Cham (2017). https://doi.org/10.1007/978-3-319-67639-5

7. Mostafa, A.E., Zhou, Y., Wong, V.W.S.: Connection density maximization of narrowband IoT systems with NOMA. IEEE Trans. Wireless Commun. **18**(10), 4708–4722 (2019)
8. Wu, F., et al.: An enhanced random access algorithm based on the clustering-reuse preamble allocation in NB-IoT system. IEEE Access. **7**, 183847–183859 (2019)
9. Xu, W., Campbell, G.: A near perfect stable random access protocol for a broadcast channel. In: Proceedings of Discovering New World Communication (SUPERCOMM/ICC), pp. 370–374. IEEE Press, Chicago (1992)
10. Zhang, X., Campbell, G.: Performance analysis of distributed queueing random access protocol–DQRAP. DQRAP Research Group report 93-1 (1994)
11. Tuset-Peiro, P., Vazquez-Gallego, F., Alonso-Zarate, J., et al.: LPDQ: a self-scheduled TDMA MAC protocol for one-hop dynamic low-power wireless networks. Pervasive Mobile Comput. **20**, 84–99 (2015)
12. Zhang, K., Marchiori, A.: Crowdsourcing low-power wide-area IoT networks. In: Proceedings of the IEEE International Conference on Pervasive Computing and Communications (PerCom), pp. 41–49. IEEE Press, Kona (2017)
13. Wu, W., Li, Y., Zhang, Y., et al.: Distributed queueing based random access protocol for LoRa networks. IEEE IoT J. **7**(1), 763–772 (2020)
14. SX1272/3/6/7/8 LoRa Modem Design Guide AN1200.13 Revision 1 (2013)
15. Reynders, B., Meert, W., Pollin, S.: Power and spreading factor control in low power wide area networks. In: 2017 IEEE International Conference on Communications (ICC), pp. 1–6. IEEE Press, Paris (2017)
16. El-Aasser, M., Elshabrawy, T., Ashour, M.: Joint spreading factor and coding rate assignment in LoRaWAN networks. In: 2018 IEEE Global Conference on Internet of Things (GCIoT), pp. 1–7. IEEE Press, Alexandria (2018)
17. Su, B., Qin, Z., Ni, Q.: Energy efficient resource allocation for uplink LoRa networks. In: 2018 IEEE Global Communications Conference (GLOBECOM), pp. 1–7. IEEE Press, Abu Dhabi (2018)
18. Amichi, L., Kaneko, M., Rachkidy, N. E., et al.: Spreading factor allocation strategy for LoRa networks under imperfect orthogonality. In: 2019 IEEE International Conference on Communications (ICC), pp. 1–7. IEEE Press, Shanghai (2019)
19. Amichi, L., Kaneko, M., Fukuda, E.H., et al.: Joint allocation strategies of power and spreading factors with imperfect orthogonality in LoRa networks. IEEE Trans. Commun. **68**(6), 3750–3765 (2020)
20. Waret, A., Kaneko, M., Guitton, A., et al.: LoRa throughput analysis with imperfect spreading factor orthogonality. IEEE Wireless Commun. Lett. **8**, 408–411 (2019)
21. Gu, Y., Saad, W., Bennis, M., et al.: Matching theory for future wireless networks: fundamentals and applications. IEEE Commun. Mag. **53**, 52–59 (2015)
22. Laporte-Fauret, B., Temim, M.A.B., Ferre, G., et al.: An enhanced LoRa-like receiver for the simultaneous reception of two interfering signals. In: 2019 IEEE 30th Annual International Symposium on Personal, Indoor and Mobile Radio Communications (PIMRC), pp. 1–6, Istanbul (2019)